INTERNATIONAL JOURNAL OF ROBUST AND NONLINEAR CONTROL
Int. J. Robust Nonlinear Control (in press)
Published online in Wiley InterScience (www.interscience.wiley.com). DOI: 10.1002/rnc.1225

High-order sliding-mode observer for a quadrotor UAV

A. Benallegue[1,*,†], A. Mokhtari[2] and L. Fridman[3]

[1] *Laboratoire d'Ingenierie des Systemes de Versailles, 10–12 avenue de l'Europe 78140 Velizy, France*
[2] *University of Science and Technology, Oran, Algeria*
[3] *Engineering Faculty, National Autonomous University of Mexico, Mexico City, Mexico*

SUMMARY

In this paper, a feedback linearization-based controller with a high-order sliding mode observer running parallel is applied to a quadrotor unmanned aerial vehicle. The high-order sliding mode observer works as an observer and estimator of the effect of the external disturbances such as wind and noise. The whole observer–estimator–control law constitutes an original approach to the vehicle regulation with minimal number of sensors. Performance issues of the controller–observer are illustrated in a simulation study that takes into account parameter uncertainties and external disturbances. Copyright © 2007 John Wiley & Sons, Ltd.

Received 1 May 2006; Revised 26 March 2007; Accepted 2 April 2007

KEY WORDS: high-order sliding mode; nonlinear control; feedback linearization; UAV

1. INTRODUCTION

1.1. Motivation

Small unmanned aerial vehicle (UAV) quadrotors are designed to easily move in different environments while following specific tasks and providing a good performance as well as a great autonomy. Affected by aerodynamic forces, the quadrotor dynamics is nonlinear, multivariable, and is subject to parameter uncertainties and external disturbances. In turn, controlling of the quadrotor is required: (i) to meet the stability, robustness and desired dynamic properties; (ii) to be able to handle nonlinearity; and (iii) to be adaptive to changing parameters and environmental disturbances.

Main difficulties of the motion control are thus parametric uncertainties, unmodelled dynamics, and external disturbances [1], which result in further complication in the design of controllers for actual systems [2, 3]. Various advanced control methods such as feedback linearization method [4] have been developed to meet increasing demands on the performance;

*Correspondence to: A. Benallegue, Laboratoire d'Ingenierie des Systemes de Versailles, 10–12 avenue de l'Europe 78140 Velizy, France.
† E-mail: benalleg@lisv.uvsq.fr

however, they required full information on the state that may limit their practical utility. Indeed, even if all the state measurements are possible they are typically corrupted by noise. Moreover, the increased number of sensors makes the overall system more complex in implementation and expensive in realization. In order to decrease the number of sensors in [5] the use of only a rotational motion sensors is proposed in order to control tilt angles and evaluate translational motion. However, aerodynamic forces still cause difficulties to overcome. Thus motivated, an observer-based feedback design becomes an attractive approach to robotic control.

The use of state observers appears to be useful not only in system monitoring and regulation but also in detecting as well as identifying failures in dynamic systems. Almost all observer designs are based on the mathematical model of the plant, is not linearized and consequently have uncertain inputs. On the other hand, the relative degree of the model with respect to the known outputs heavily depend on the accuracy of the mathematical model of the plant [6].

So the main motivations of the paper are: first, the use of observer to avoid the third derivatives of the measured states needed for the feedback linearization controller of the quadrotor, second, when the quadrotor is subjected to external disturbances, it would be suitable to compensate them through an observer-based controller, third, the observer should be robust with respect to external perturbations (wind and noise) and finally, observers-based identification perturbation allows to reduce the number of sensors required for control design.

1.2. Methodology

Sliding mode observers (see, for example, the corresponding chapters in the textbooks [7, 8], and the recent tutorials [9–11]) are widely used due to their attractive features: (a) insensitivity (more than robustness!) with respect to unknown inputs; (b) possibilities to use the values of the equivalent output injection for the unknown inputs identification; and (c) finite-time convergence to exact values of the state vectors.

In [12–14] a robust exact arbitrary order differentiator was designed ensuring finite-time convergence to the values of the corresponding derivatives, and applications of higher-order sliding algorithms were considered.

Modifying the second-order sliding-mode supertwisting algorithm, Davila *et al.* [15, 16] proposed an observer for mechanical systems with only position measurements ensuring best possible approximation for the velocities and uncertainties.

The relative degree of the UAV quadrotors model w.r.t. unknown inputs is 2 or 4 and the standard necessary and sufficient conditions for observation of the systems with unknown inputs without differentiation are not fulfilled [17]. To solve the problem of observation for UAV quadrotors the higher-order sliding-mode observers based on higher-order sliding-mode differentiation [14] will be used.

1.3. Main contribution

In the paper the models of UAV quadrotor and feedback linearization-based controller are suggested. To realize this with a high-order sliding-mode observer running parallel is applied to a quadrotor UAV. The high-order sliding-mode observer works as an observer and estimator of the effect of the external disturbances such as wind and noise. To realize the control algorithm and identify the uncertainties a fourth-order sliding-mode observer based on third-order

DOI: 10.1002/rnc

differentiator robust exact differentiator [14] is suggested. This observer ensures the identification of the wind and noise effect. The whole observer–estimator–control law constitutes an original approach to the vehicle regulation with minimal number of sensors. Performance issues of the controller–observer are illustrated in a simulation study that takes into account parameter uncertainties and external disturbances.

1.4. *Paper structure*

The rest of the paper is outlined as follows. UAV dynamics is deduced in Section 2. The inner outer controller is developed in Section 3. The observer design is presented in Section 4. Simulation results are given in Section 5. Section 6 yields some conclusions.

2. QUADROTOR DYNAMICS

The quadrotor is composed of four rotors. Two diagonal motors (1 and 3) are running in the same direction whereas the others (2 and 4) in the other direction to eliminate the anti-torque. On varying the rotor speeds altogether with the same quantity the lift forces will change affecting in this case the altitude z of the system and enabling vertical take-off/on landing. Yaw angle ψ is obtained by speeding up/slowing down the diagonal motors depending on the desired direction. Roll angle ϕ axe allows the quadrotor to move towards y direction. Pitch angle θ axe allows the quadrotor to move towards x direction. The rotor is the primary source of control and propulsion for the UAV. The Euler angle orientation to the flow provides the forces and moments to control the altitude and position of the system. The absolute position is described by three coordinates (x_0, y_0, z_0), and its attitude by Euler angles (ψ, θ, ϕ), under the conditions $(-\pi \leqslant \psi < \pi)$ for yaw, $(-\pi/2 < \theta < \pi/2)$ for pitch, and $(-\pi/2 < \phi < \pi/2)$ for roll (Figure 1).

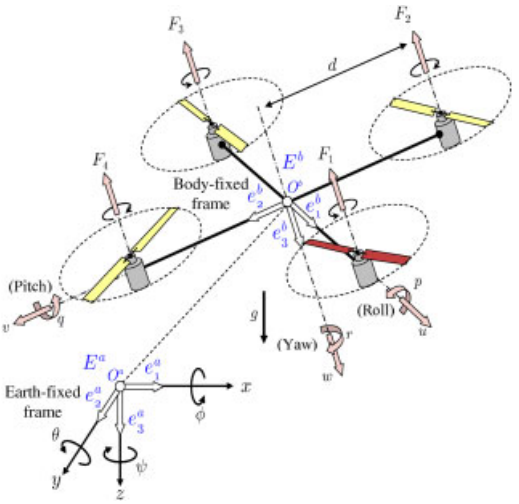

Figure 1. The quadrotor helicopter.

DOI: 10.1002/rnc

The derivatives with respect to time of the angles (ψ, θ, ϕ) can be expressed in the form

$$\mathrm{col}(\dot{\psi}, \dot{\theta}, \dot{\phi}) = \begin{bmatrix} 0 & S\phi S_e\theta & C\phi S_e\theta \\ 0 & C\phi & -S\phi \\ 1 & S\phi T\theta & C\phi T\theta \end{bmatrix} \omega \tag{1}$$

with $S. = \sin(\cdot)$, $C. = \cos(\cdot)$, $T. = \tan(\cdot)$, $S_e. = \sec(\cdot)$ and $\omega = \mathrm{col}(p, q, r)$ is the angular velocity expressed with respect to a body reference frame.

Similarly, the time derivative of the position (x_0, y_0, z_0) is given by

$$\mathrm{col}(\dot{x}_0, \dot{y}_0, \dot{z}_0) = V_0 \tag{2}$$

where $V_0 = \mathrm{col}(u_0, v_0, w_0)$ is the absolute velocity of the UAV expressed with respect to an earth fixed inertial reference frame.

Equations (1) and (2) are the kinematic equations. The dynamic equations are now expressed. Using Newton's laws about the centre of mass one obtains the dynamic equations for the miniature four rotors helicopter

$$m\dot{V}_0 = \sum F_{\mathrm{ext}} \tag{3}$$

$$J\dot{\omega} = -\omega \times J\omega + \sum T_{\mathrm{ext}} \tag{4}$$

where the symbol $\times$ denotes the usual vector product, m is the mass, J is the inertia matrix which is given by

$$J = \mathrm{diag}(I_x, I_y, I_z)$$

Due to the symmetry of the geometric form of the quadrotor the coupling inertia is assumed to be zero. The notations $\sum F_{\mathrm{ext}}$, $\sum T_{\mathrm{ext}}$ stand for the vector of external forces and that of external torques, respectively. They contain the helicopter's weight, the aerodynamic forces vector, the thrust and the torque developed by the four rotors. It is straightforward to compute that

$$\sum F_{\mathrm{ext}} = \begin{bmatrix} A_x - (C\phi C\psi S\theta + S\phi S\psi)u_1 \\ A_y - (C\phi S\theta S\psi - C\psi S\phi)u_1 \\ A_z + mg - (C\theta C\phi)u_1 \end{bmatrix}, \quad \sum T_{\mathrm{ext}} = \begin{bmatrix} A_p + u_2 d \\ A_q + u_3 d \\ A_r + u_4 \end{bmatrix} \tag{5}$$

- $[A_x, A_y, A_z]^{\mathrm{T}}$ and $[A_p, A_q, A_r]^{\mathrm{T}}$ are the resulting aerodynamic forces and moments acting on the UAV and are computed from the aerodynamic coefficients C_i as $A_i = \frac{1}{2}\rho_{\mathrm{air}} C_i W^2$ [18, 19] (ρ_{air} is the air density, W is the velocity of the UAV with respect to the air) [20]. (C_i depends on several parameters like the angle between airspeed and the body fixed reference system, the aerodynamic and geometric form of the wing);
- g is the gravity constant ($g = 9.81\ \mathrm{m/s^2}$);
- d is the distance from the centre of mass to the rotors;
- $u_1 = (F_1 + F_2 + F_3 + F_4)$ is the resulting thrust of the four rotors;
- $u_2 = d(F_4 - F_2)$ is the difference of thrust between the left rotor and the right rotor;
- $u_3 = d(F_3 - F_1)$ is the difference of thrust between the front rotor and the back rotor;

DOI: 10.1002/rnc

- $u_4 = C(F_1 - F_2 + F_3 - F_4)$ is the difference of torque between the two clockwise turning rotors and the two counter-clockwise turning rotors;
- C is the force to moment scaling factor.

Assuming that the electric motors are velocity controlled, then (u_1, u_2, u_3, u_4) may be viewed as control inputs. The dynamic model of the quadrotor has been developed in many experimental works but in different manners, like Bouabdallah *et al.* [21]. With reference to [22], the real control signals (u_1, u_2, u_3, u_4) have been replaced by $(\bar{u}_1, \bar{u}_2, \bar{u}_3, \bar{u}_4)$ to avoid singularity in Lie transformation matrices when using exact linearization. In that case u_1 has been delayed by double integrator. The other control signals will remain unchanged

$$\begin{aligned} u_1 &= \zeta, \quad \dot{\zeta} = \xi, \quad \dot{\xi} = \bar{u}_1 \\ u_2 &= \bar{u}_2 \\ u_3 &= \bar{u}_3 \\ u_4 &= \bar{u}_4 \end{aligned} \tag{6}$$

The obtained extended system is described by state-space equations of the form

$$\begin{aligned} \dot{x} &= \bar{f}(x) + \sum_{i=1}^{4} \bar{g}_i(x)\bar{u}_i \\ y &= h(x) \end{aligned} \tag{7}$$

where $x = [x_0, y_0, z_0, \psi, \theta, \phi, u_0, v_0, w_0, \zeta, \xi, p, q, r]^{\mathrm{T}}$, $y = [x_0, y_0, z_0, \psi]^{\mathrm{T}}$ and

$$\bar{f} = \begin{bmatrix} u_0 \\ v_0 \\ w_0 \\ qS\phi S_e\theta + rC\phi S_e\theta \\ qC\phi - rS\phi \\ p + qS\phi T\theta + rC\phi T\theta \\ \dfrac{Ax}{m} - \dfrac{1}{m}(C\phi C\psi S\theta + S\phi S\psi)\zeta \\ \dfrac{A_y}{m} - \dfrac{1}{m}(C\phi S\theta S\psi - C\psi S\phi)\zeta \\ \dfrac{A_z}{m} + g - \dfrac{1}{m}(C\theta C\phi)\zeta \\ \xi \\ 0 \\ \dfrac{I_y - I_z}{I_x}qr + \dfrac{A_p}{Ix} \\ \dfrac{I_z - I_x}{I_y}pr + \dfrac{A_q}{Iy} \\ \dfrac{I_x - I_y}{I_z}pq + \dfrac{A_r}{Iz} \end{bmatrix}, \quad \begin{aligned} \bar{g}_1(x) &= [0,0,0,0,0,0,0,0,0,0,1,0,0,0]^{\mathrm{T}} \\ \bar{g}_2(x) &= \left[0,0,0,0,0,0,0,0,0,0,0,\frac{d}{I_x},0,0\right]^{\mathrm{T}} \\ \bar{g}_3(x) &= \left[0,0,0,0,0,0,0,0,0,0,0,\frac{d}{I_y},0\right]^{\mathrm{T}} \\ \bar{g}_4(x) &= \left[0,0,0,0,0,0,0,0,0,0,0,0\frac{1}{I_z}\right]^{\mathrm{T}} \end{aligned}$$

DOI: 10.1002/rnc

The purpose of the next section is to design a feedback controller for the four-rotor miniature helicopter which exhibits robustness properties against neglected effects and parametric uncertainties.

3. FEEDBACK LINEARIZATION CONTROLLER

The feedback linearization technique is based on inner and outer loops of the controller. The input–output linearization-based inner loop uses the full-state feedback to globally linearize the nonlinear dynamics of selected controlled outputs. Each of the output channels is differentiated sufficiently many times until a control input component appears in the resulting equation. Using the Lie derivative, input–output linearization will transform the nonlinear system into a linear and non-interacting system in the Brunovsky form. The outer controller adopts a classical polynomial control law for the new input variable of the resulting linear system.

3.1. Structure of the inner controller

The input–output decoupling problem is solvable for the nonlinear system (7) by means of static feedback. The vector relative degree $\{r_1, r_2, r_3, r_4\}$ is given by $r_1 = r_2 = r_3 = 4$ and $r_4 = 2$ and we have

$$\mathrm{col}(y_1^{(r_1)}, y_2^{(r_2)}, y_3^{(r_3)}, y_4^{(r_4)}) = b(x) + \Delta(x)\bar{u} \tag{8}$$

where $b(x)$ and $\Delta(x)$ are computed as follows:

$$b(x) = \begin{bmatrix} L_f^{r_1} h_1(x) \\ \vdots \\ L_f^{r_4} h_4(x) \end{bmatrix}, \quad \Delta(x) = \begin{bmatrix} L_{g_1} L_f^{r_1-1} h_1(x) & \cdots & L_{g_4} L_f^{r_1-1} h_1(x) \\ \vdots & \ddots & \vdots \\ L_{g_1} L_f^{r_4-1} h_4(x) & \cdots & L_{g_4} L_f^{r_4-1} h_4(x) \end{bmatrix} \tag{9}$$

where

$$L_f h(x) = \sum_{i=1}^{n} \frac{\partial h}{\partial x_i} f_i(x) \quad \text{and} \quad L_f^k h(x) = L_f(L_f^{k-1} h(x))$$

The matrix $\Delta(x)$ is non-singular everywhere in the region $\zeta \neq 0$, $-\pi/2 < \phi < \pi/2$, $-\pi/2 < \theta < \pi/2$. Therefore, the input–output decoupling problem is solvable for system (7) by means of a control law of the form

$$\bar{u} = \Delta^{-1}(x)(-b(x) + v) \tag{10}$$

Moreover, since system (7) has dimension $n = 14$, the condition $r_1 + r_2 + r_3 + r_4 = n$ is fulfilled and therefore, the system can be transformed *via* static feedback into a system which, in suitable coordinates, is fully linear and controllable. However, due to the presence of external disturbances the input–output linearization is not exact and the inner closed-loop system in that

DOI: 10.1002/rnc

case is composed into a linear part and a nonlinear disturbance part

$$\begin{pmatrix} y_1^{(4)} \\ y_2^{(4)} \\ y_3^{(4)} \\ y_4^{(2)} \end{pmatrix} = \begin{pmatrix} \dfrac{\mathrm{d}^4 x_0}{\mathrm{d}t^4} \\ \dfrac{\mathrm{d}^4 y_0}{\mathrm{d}t^4} \\ \dfrac{\mathrm{d}^4 z_0}{\mathrm{d}t^4} \\ \dfrac{\mathrm{d}^2 \psi}{\mathrm{d}t^2} \end{pmatrix} = \begin{pmatrix} v_1 \\ v_2 \\ v_3 \\ v_4 \end{pmatrix} + \begin{pmatrix} \xi_1(x,t) \\ \xi_2(x,t) \\ \xi_3(x,t) \\ \xi_4(x,t) \end{pmatrix} \tag{11}$$

with

$$\begin{pmatrix} \xi_1(x,t) \\ \xi_2(x,t) \\ \xi_3(x,t) \\ \xi_4(x,t) \end{pmatrix} = \begin{pmatrix} \dfrac{\ddot{A}_x}{m} + a_{14}A_p + a_{15}A_q \\ \dfrac{\ddot{A}_y}{m} + a_{24}A_p + a_{25}A_q \\ \dfrac{\ddot{A}_z}{m} + a_{34}A_p + a_{35}A_q \\ a_{45}A_q + a_{46}A_r \end{pmatrix}$$

where

$$\begin{aligned} a_{14} &= (\zeta S\phi C\psi S\theta - \zeta C\phi S\psi)/(mI_x), \quad a_{15} = -(\zeta C\psi C\theta)/(mI_y) \\ a_{24} &= (\zeta S\phi S\psi S\theta + \zeta C\phi C\psi)/(mI_x), \quad a_{25} = -(\zeta S\psi C\theta)/(mI_y) \\ a_{34} &= (\zeta S\phi C\theta)/(mI_x), \quad a_{35} = (\zeta S\theta)(mI_y) \\ a_{45} &= S\phi/(I_y C\theta), \quad a_{46} = C\phi/(I_z C\theta) \end{aligned}$$

v_1, v_2, v_3, v_4, represent the new input control signals. The controller compares the primary state (x_0, y_0, z_0, ψ) and their successive derivatives to the desired state trajectory.

3.2. Structure of the outer controller

While adapting a classical polynomial control law for the new input variable v with disturbance compensation, one obtains the following equations:

$$\begin{aligned} v_1 &= x_d^{(4)} - \lambda_3 \dddot{e}_{11} - \lambda_2 \ddot{e}_{11} - \lambda_1 \dot{e}_{11} - \lambda_0 e_{11} - z_{41}^f \\ v_2 &= y_d^{(4)} - \lambda_3 \dddot{e}_{12} - \lambda_2 \ddot{e}_{12} - \lambda_1 \dot{e}_{12} - \lambda_0 e_{12} - z_{42}^f \\ v_3 &= z_d^{(4)} - \lambda_3 \dddot{e}_{13} - \lambda_2 \ddot{e}_{13} - \lambda_1 \dot{e}_{13} - \lambda_0 e_{13} - z_{43}^f \\ v_4 &= \ddot{\psi}_d - \lambda_5 \dot{e}_5 - \lambda_4 e_5 - z_6^f \end{aligned} \tag{12}$$

where x_d, y_d, z_d, ψ_d represent the desired output signals, corresponding to x_0, y_0, z_0, ψ, respectively, the error signals $e_{11} = [x_0 - x_{0d}]$, $e_{12} = [y_0 - y_{0d}]$, $e_{13} = [z_0 - z_{0d}]$, and $e_5 = [\psi - \psi_d]$ and the coefficients λ_i, $i = 0, \ldots, 5$ are to be specified in the sequel. The variables

DOI: 10.1002/rnc

z_{41}^f, z_{42}^f, z_{43}^f, and z_6^f are the filtered signals of z_{41}, z_{42}, z_{43}, and z_6 given in the observer section. The closed-loop system (11), (12) can be rewritten in the form

$$\dot{e} = Ae + \tilde{\xi}(x,t)$$

$$\tilde{\xi} = \xi - z^f = [\xi_1, \xi_2, \xi_3, \xi_4]^{\mathrm{T}} - [z_{41}^f, z_{42}^f, z_{43}^f, z_6^f]^{\mathrm{T}}$$

where e represents the tracking error between the desired value and the actual one given by $e = [e_1, e_2, e_3, e_4, e_5, e_6]^{\mathrm{T}}$, $e_1 = [e_{11}, e_{12}, e_{13}]^{\mathrm{T}}$, $e_2 = \dot{e}_1$, $e_3 = \ddot{e}_1$, $e_4 = \dddot{e}_1$, and $e_6 = \dot{e}_5$. The vector $\tilde{\xi}(x,t)$ is the wind parameter errors of the disturbances and the matrix A is then given by

$$A = \begin{bmatrix} 0 & I & 0 & 0 & 0 & 0 \\ 0 & 0 & I & 0 & 0 & 0 \\ 0 & 0 & 0 & I & 0 & 0 \\ -\lambda_0 I & -\lambda_1 I & -\lambda_2 I & -\lambda_3 I & 0 & 0 \\ 0 & 0 & 0 & 0 & 0 & 1 \\ 0 & 0 & 0 & 0 & -\lambda_4 & -\lambda_5 \end{bmatrix}$$

where I is an identity matrix of dimension 3×3 and the control gains λ_i, $i = 0, \ldots, 5$ are such that the eigenvalues of the matrix A have desired locations.

It is very important to know the domain of attraction of an equilibrium point, that is the set of initial states from which the system converges to the equilibrium point itself [23, 24]. Actually, such problem arises in both system analysis and synthesis, in order to guarantee a stable behaviour in a certain region of the state space.

4. HIGH-ORDER SLIDING-MODE OBSERVER

The navigation sensor package will include a differential global positioning system (DGPS) which provides high-accuracy position and velocity information. For the x- and y-positions, the DGPS provides both the proportional and derivative terms. To compensate for poor GPS accuracy in the vertical direction, a sonar altimeter (based on ultrasonic transducer) will be employed to provide altitude information at a reasonable accuracy. A digital compass will be used to establish the helicopter yaw angle to about $\pm 1^\circ$. While the navigation sensors and the associated inner-loop control software are able to have the helicopter take-off, land, and fly from waypoint to waypoint, the UAV must be capable of establishing these waypoints. Since the competition environment is dynamic, this must be done in real time [25].

Motivated by practice, the measured UAV variables are the absolute positions x_0, y_0, z_0 and the orientation ψ which represent the translational motion and rotation around the z-axis, respectively. Although non-measurable signals can be obtained by successive differentiation, however, they are contaminated by the measurement noise to such a degree that the differentiation can no longer be used. To avoid numerical differentiation let us construct an observer based on arbitrary order high-order sliding-mode differentiator [14].

DOI: 10.1002/rnc

4.1. Observer model

The linearized dynamic model of the quadrotor with the measured signals $x_1 = [x_0, y_0, z_0]^{\mathrm{T}}$, and $x_5 = \psi$ can be represented in the following state-space form:

$$\begin{aligned}
\dot{x}_1 &= x_2 \\
\dot{x}_2 &= x_3 \\
\dot{x}_3 &= x_4 \\
\dot{x}_4 &= [v_1, v_2, v_3]^{\mathrm{T}} + [\xi_1, \xi_2, \xi_3]^{\mathrm{T}} \\
\dot{x}_5 &= x_6 \\
\dot{x}_6 &= v_4 + \xi_4
\end{aligned} \tag{13}$$

Let us propose the observer based on high-order differentiation for the state variables $x_1, x_2, x_3, x_4, x_5, x_6$ of the form

$$\begin{aligned}
\dot{\hat{x}}_1 &= \hat{x}_2 + \gamma_1 |x_1 - \hat{x}_1|^{3/4} \operatorname{sign}(x_1 - \hat{x}_1) \\
\dot{\hat{x}}_2 &= \hat{x}_3 + \gamma_2 |\mu_2 - \hat{x}_2|^{2/3} \operatorname{sign}(\mu_2 - \hat{x}_2) \\
\dot{\hat{x}}_3 &= \hat{x}_4 + \gamma_3 |\mu_3 - \hat{x}_3|^{1/2} \operatorname{sign}(\mu_3 - \hat{x}_3) \\
\dot{\hat{x}}_4 &= [v_1, v_2, v_3]^{\mathrm{T}} + z_4 \\
\dot{\hat{x}}_5 &= \hat{x}_6 + \gamma_4 |x_5 - \hat{x}_5|^{1/2} \operatorname{sign}(x_5 - \hat{x}_5) \\
\dot{\hat{x}}_6 &= v_4 + z_6
\end{aligned} \tag{14}$$

where

$$\begin{aligned}
z_4 &= \alpha_4 \operatorname{sign}(\mu_4 - \hat{x}_4) \\
z_6 &= \alpha_6 \operatorname{sign}(\mu_6 - \hat{x}_6)
\end{aligned} \tag{15}$$

and $\mu_2 = \hat{x}_2 + z_1$, $\mu_3 = \hat{x}_3 + z_2$, $\mu_4 = \hat{x}_4 + z_3$, $\mu_6 = \hat{x}_6 + z_5$.

Theorem 1

The observer (14), (15) for system (13) ensures in finite time the convergence of the estimated states to the real states, i.e. $(\hat{x}_1, \hat{x}_2, \hat{x}_3, \hat{x}_4, \hat{x}_5, \hat{x}_6) \to (x_1, x_2, x_3, x_4, x_5, x_6)$. The filtered values of $z_4^f = [z_{41}^f, z_{42}^f, z_{43}^f]^{\mathrm{T}}$ and z_6^f converge to $\xi_{123} = [\xi_1, \xi_2, \xi_3]^{\mathrm{T}}$ and ξ_4 in the intervals of differentiability of ξ_{123} and ξ_4 when the filter time constant match more than sampling step and both tend to zero.

Proof

The finite-time convergence of observers for variables $\tilde{x}_5, \tilde{x}_6$ is proved in [15]. Taking $\tilde{x}_i = x_i - \hat{x}_i$ the estimation error can be written as

$$\begin{aligned}
\dot{\tilde{x}}_1 &= \tilde{x}_2 - \gamma_1 |\tilde{x}_1|^{3/4} \operatorname{sign}(\tilde{x}_1) \\
\dot{\tilde{x}}_2 &= \tilde{x}_3 - \gamma_2 |\mu_2 - \hat{x}_2|^{2/3} \operatorname{sign}(\mu_2 - \hat{x}_2)
\end{aligned}$$

DOI: 10.1002/rnc

$$\dot{\tilde{x}}_3 = \tilde{x}_4 - \gamma_3|\mu_3 - \hat{x}_3|^{1/2}\text{sign}(\mu_3 - \hat{x}_3)$$
$$\dot{\tilde{x}}_4 = \xi_{123} - \alpha_4\,\text{sign}(\mu_4 - \hat{x}_4) \tag{16}$$

To prove finite-time convergence of the error of observer (14) for $\tilde{x}_1, \tilde{x}_2, \tilde{x}_3, \tilde{x}_4$, we just need to rewrite first four equations of (16) in the form of differential inclusion

$$\dot{\tilde{x}}_1 = \tilde{x}_2 - \gamma_1|\tilde{x}_1|^{3/4}\,\text{sign}(\tilde{x}_1)$$
$$\dot{\tilde{x}}_2 = \tilde{x}_3 - \gamma_2|\mu_2 - \hat{x}_2|^{2/3}\,\text{sign}(\mu_2 - \hat{x}_2)$$
$$\dot{\tilde{x}}_3 = \tilde{x}_4 - \gamma_3|\mu_3 - \hat{x}_3|^{1/2}\,\text{sign}(\mu_3 - \hat{x}_3)$$
$$\dot{\tilde{x}}_4 \in [-f_4^+, f_4^+] - \alpha_4\,\text{sign}(\mu_4 - \hat{x}_4) \tag{17}$$

This inclusion is understood in Filippov sense [26]. The proof of finite-time convergence now follows from Lemma 8 in [14]. The convergence of the filtered values of $z_4^f = [z_{41}^f, z_{42}^f, z_{43}^f]^{\mathrm{T}}$ and z_6^f to $\xi_{123} = [\xi_1, \xi_2, \xi_3]^{\mathrm{T}}$ and ξ_4 in the intervals of differentiability of ξ_{123} and ξ_4 follows from the theorem about physical meaning of equivalent control [27] (Chapter 2). □

4.2. Output states reconstruction

The sliding observer presented above is in fact a state estimator with partial state feedback (x_0, y_0, z_0, ψ) taken as measured variables. The observer estimates the state needed by the control law to calculate the tracking error between the desired trajectories $(x_{1d}, x_{2d}, x_{3d}, x_{4d}, x_{5d}, x_{6d})$ and the estimated ones $(\hat{x}_1, \hat{x}_2, \hat{x}_3, \hat{x}_4, \hat{x}_5, \hat{x}_6)$. Unfortunately, the estimated state does not involve all the output states. In that case, to complete the full state output, the missed variables (θ, ϕ, p, q, r) of the state vector x (7) have been calculated through the estimated values and from the nonlinear system of Equation (7), without taking the perturbation into account. So, from (7) θ and ϕ are deduced as follows:

$$\hat{\phi} = \arcsin\left(\frac{-m(\hat{\ddot{x}}_0 S\psi - \hat{\ddot{y}}_0 C\psi)}{\zeta}\right), \quad \hat{\theta} = \frac{1}{C\hat{\phi}}\arcsin\left(\frac{-m(\hat{\ddot{x}}_0 C\psi + \hat{\ddot{y}}_0 S\psi)}{\zeta}\right) \tag{18}$$

The variables $(\hat{p}, \hat{q}, \hat{r})$ can be found from the transformation equation (1) which needs the variables $(\dot{\hat{\psi}}, \dot{\hat{\theta}}, \dot{\hat{\phi}})$. The latter can be evaluated from (18) and the third derivatives $(\dddot{\hat{x}}_0, \dddot{\hat{y}}_0)$, i.e.

$$\dot{\hat{\theta}} = -\frac{1}{C\hat{\theta}C^2\hat{\phi}\zeta}\{m\,\dddot{\hat{x}}_0(S\hat{\phi}S\hat{\theta}S\psi + C\psi C\hat{\phi}) + m\,\dddot{\hat{y}}_0(C\hat{\phi}S\psi - S\hat{\phi}C\psi S\hat{\theta}) + \dot{\hat{\psi}}\zeta C\hat{\phi}S\hat{\phi}C^2\hat{\theta} - S\hat{\theta}\zeta\}$$

$$\dot{\hat{\phi}} = \frac{1}{\zeta C(\hat{\phi})}\{-m\,\dddot{\hat{x}}_0 S\psi + \psi\zeta C\hat{\phi}S\hat{\theta} + \zeta S\hat{\phi} + mC\psi\,\dddot{\hat{y}}_0\}$$

DOI: 10.1002/rnc

So from the following matrix equation, the estimation of the variables $(\hat{p}, \hat{q}, \hat{r})$ can be deduced:

$$\begin{bmatrix} \hat{p} \\ \hat{q} \\ \hat{r} \end{bmatrix} = \begin{bmatrix} 0 & S\hat{\phi}S_e\hat{\theta} & C\hat{\phi}S_e\hat{\theta} \\ 0 & C\hat{\phi} & -S\hat{\phi} \\ 1 & S\hat{\phi}T\hat{\theta} & C\hat{\phi}T\hat{\theta} \end{bmatrix}^{-1} \begin{bmatrix} \dot{\hat{\psi}} \\ \dot{\hat{\theta}} \\ \dot{\hat{\phi}} \end{bmatrix} \tag{19}$$

The stability proof for this overall closed-loop system is similar to those of Theorem 1 and it is therefore omitted. Instead, simulation evidences will be provided in the next section.

5. SIMULATION RESULTS

The constant quadrotor parameters, used in the simulation run, are $m = 2$ kg; $I_x = I_y = 0.8$; $I_z = 1.2416$ N.m/rad/s^2; $d = 0.1$ m and $g = 9.81$ m/s^2. The gain values of $(\lambda_0, \lambda_1, \lambda_2, \lambda_3)$ and (λ_4, λ_5) represent the coefficients of the polynomial $(s+5)^4$ and $(s+5)^2$, respectively. For a specific f_i^+ and α_i, the values of γ_i are chosen as $\gamma_1 = 3$, $\gamma_2 = 2.5$, $\gamma_3 = \gamma_4 = 1.5$ and $\alpha_4 = \alpha_6 = 1.1$. An application has been established without and with disturbances and with uncertainties to test the performance and robustness of the sliding-mode observer.

- Simulation without disturbance: $(A_x = A_y = A_z = 0)$; $(A_p = A_q = A_r = 0)$; the obtained results are shown in Figure 2.
- Simulation with aerodynamic force disturbances: for $A_x = 2\sin(0.1t)$, $A_y = 2\sin(0.1t)$, $A_z = 2\sin(0.1t)$ occurring at 10, 20, and 40 s, respectively, the obtained results are shown in Figures 3–5.
- Simulation with aerodynamic moment disturbances: for $A_p = 0.09\sin(0.1t)$, $A_q = 0.01\sin(0.1t)$, $A_r = 0.2\sin(0.1t)$ occurring at 10, 20, and 40 s, respectively, the obtained results are given in Figure 6.

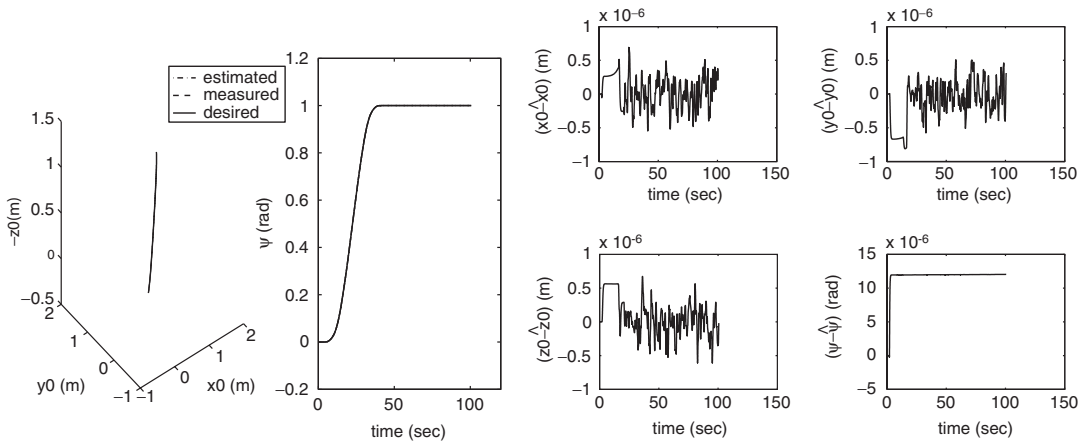

Figure 2. Reference trajectories and estimation errors.

DOI: 10.1002/rnc

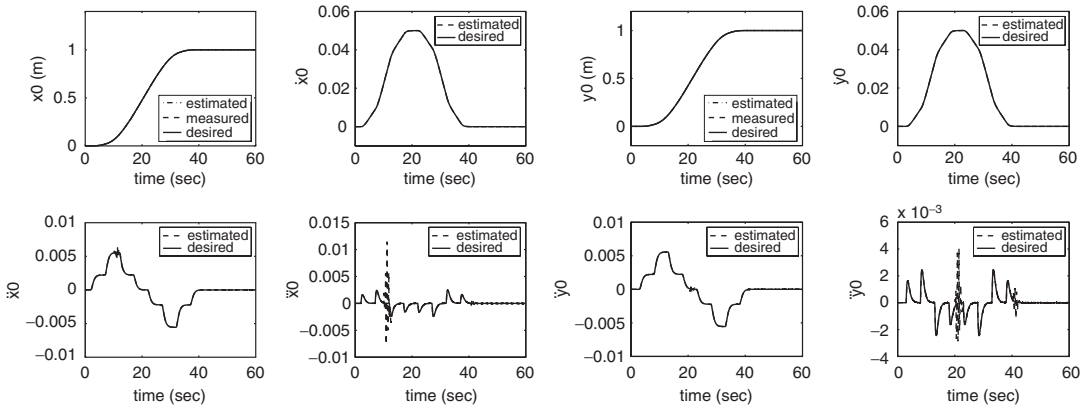

Figure 3. Trajectories x_0, $\dot{x}_0$, $\ddot{x}_0$, $\dddot{x}_0$ and trajectories y_0, $\dot{y}_0$, $\ddot{y}_0$, $\dddot{y}_0$.

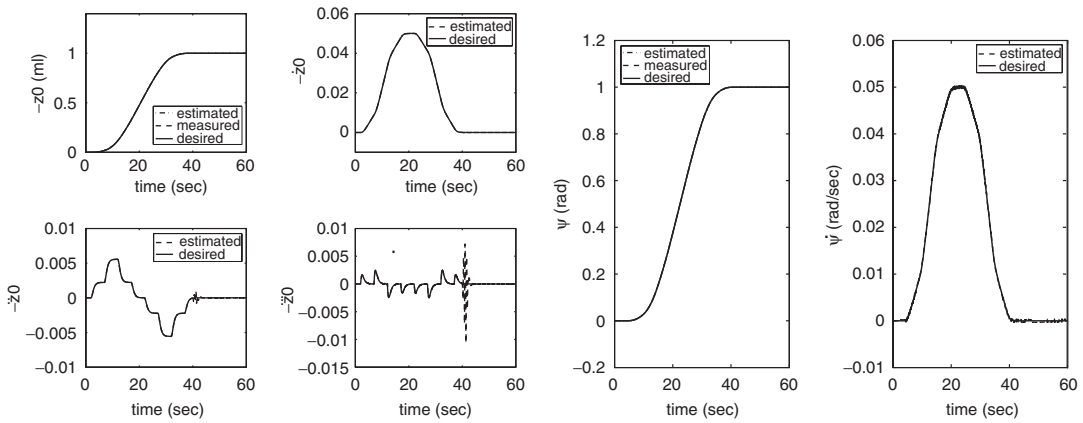

Figure 4. Trajectories z_0, $\dot{z}_0$, $\ddot{z}_0$, $\dddot{z}_0$ and trajectories ψ, $\dot{\psi}$.

It is concluded from the simulations, made without perturbation, that the high-order sliding-mode observer gives satisfactory results. The results of estimation errors given in Figure 2 show the efficiency of the observer. The same conclusion follows from the tracking errors which vanish after a finite time with a perfect convergence. When wind disturbances are introduced the results in Figures 3 and 4 reflect the robustness of the mixed observer–controller, without the need of an external estimation procedure. The estimation of force and moment disturbances are presented in Figures 5 and 6, it shows that the estimated disturbances follow exactly the computed ones. However, it appears that the system dynamic behaviour is more sensitive towards aerodynamic moment disturbances. This is also confirmed by variation of forces F_1, F_2, F_3, and F_4 in Figure 6 which exactly reflects the movement of the quadrotor in x, y, and z directions in the presence of disturbances. The convergence of the output state vector is obtained in spite of the non-robust exact linearization against uncertainties on system parameters. On the other hand, excessive chattering around desired trajectories is avoided by using high-order sliding mode.

DOI: 10.1002/rnc

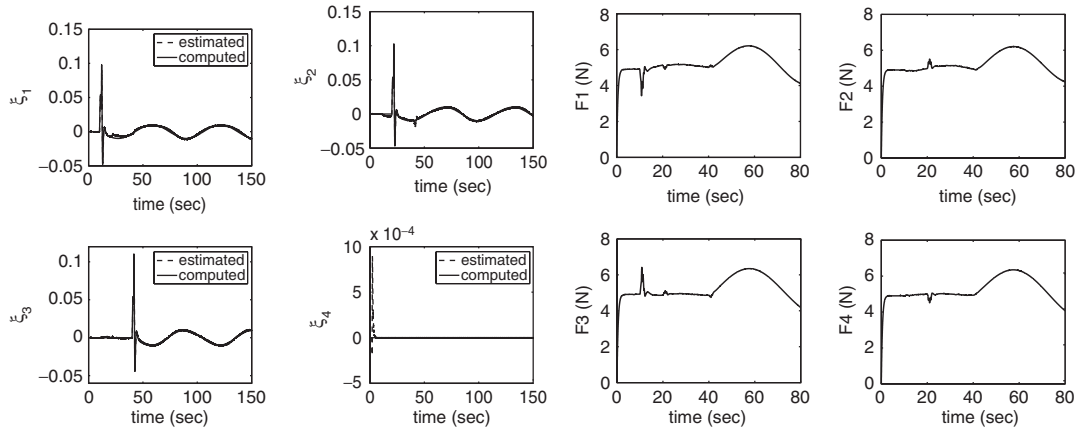

Figure 5. Disturbance estimation and applied forces with A_x, A_y, A_z.

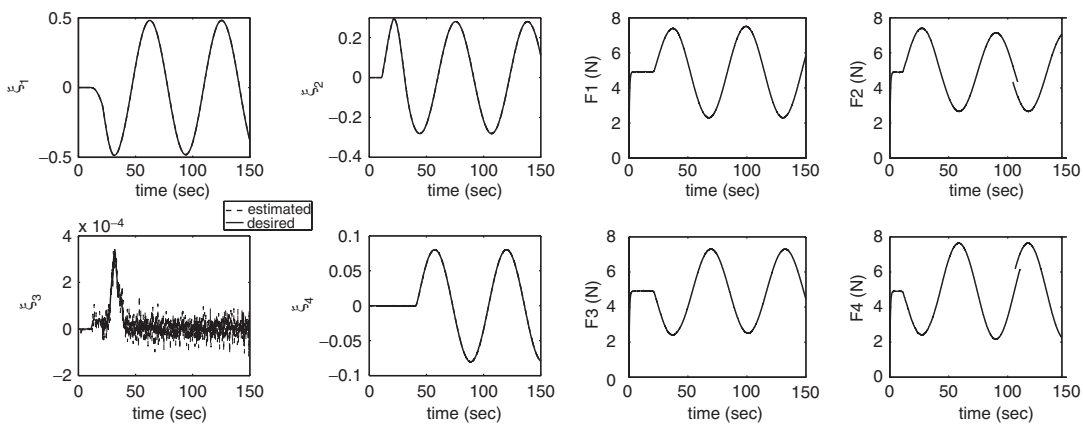

Figure 6. Disturbance estimation and applied forces with A_p, A_q, A_r.

6. CONCLUSION

A feedback linearization controller using high-order sliding-mode observer has been applied to a quadrotor unmanned aerial vehicle (UAV). Although the behaviour of the UAV, affected by aerodynamic forces and moments, is nonlinear and high coupled, the feedback linearization coupled to HOSM observer and applied to the UAV, turns out to be a good starting point to avoid complex nonlinear control solutions and excessive chattering. However, in the presence of nonlinear disturbances the system after linearization remains nonlinear. The observer used here overcomes easily this nonlinearities by an inner estimation of the external disturbances to impose desired stability and robustness properties on the global closed-loop system. The unmeasured states and their derivatives have been successfully reconstructed through the sliding-mode observer design.

DOI: 10.1002/rnc

Theoretical results have been supported by numerical simulations that demonstrated efficiency of the proposed controller design. It is hoped that further investigation would be carried out on robust controllers that would compensate noise effects and initial condition problems.

REFERENCES

1. Kim BK. Disturbance observer based approach to the design of sliding mode controller for high performance positing systems. *Fifteenth Triennial World Congress* (*IFAC*), Barcelona, 2002.
2. Jong-Rae K. Model-error control synthesis: a new approach to robust control. *Ph.D. Dissertation*, Texas A&M University, College Station, TX, August 2002.
3. Castillo P, Lozano R, Dzul A. *Modelling and Control of Mini-flying Machines*. Springer: Berlin, 2005.
4. Slotine J-JE, Hedrick JK. Robust input–output feedback linearization. *International Journal of Control* 1993; **57**:1133–1139.
5. Mokhtari A, Benallegue A. Dynamic feedback controller of Euler angles and wind parameters estimation for a quadrotor unmanned aerial vehicle. *IEEE International Conference on Robotics and Automation* (*ICRA'04*), New Orleans, U.S.A., 2004.
6. Wang W, Weiwen ZG. A comparison study of advanced state observer design techniques. *American Control Conference* (*ACC'03*), Denver, CO, June 2003.
7. Edwards C, Spurgeon S. *Sliding Mode Control*. Taylor & Francis: London, 1998.
8. Utkin V, Guldner J, Shi J. *Sliding Modes in Electromechanical Systems*. Taylor & Francis: London, 1999.
9. Barbot JP, Djemai M, Boukhobza T. Sliding mode observers. In *Sliding Mode Control in Engineering*, Perruquetti W, Barbot JP (eds). Control Engineering. Marcel Dekker: New York, 2002; 103–130.
10. Edwards C, Spurgeon S, Hebden RG. On development and applications of sliding mode observers. In *Variable Structure Systems*: *Towards XXIst Century*, Xu J, Xu Y (eds). Lecture Notes in Control and Information Science. Springer: Berlin, 2002; 253–282.
11. Poznyak A. Stochastic output noise effects in sliding mode estimations. *International Journal of Control* 2003; **76** (9–10):986–999.
12. Levant A. Sliding order and sliding accuracy in sliding mode control. *International Journal of Control* 1993; **58**: 1247–1263.
13. Levant A. Robust exact differentiation via sliding mode technique. *Automatica* 1998; **34**(3):379–384.
14. Levant A. High-order sliding modes: differentiation and output-feedback control. *International Journal of Control* 2003; **76**(9–10):924–941.
15. Davila J, Fridman L, Levant A. Second order sliding mode observer for mechanical systems. *IEEE Transactions on Automatic Control* 2005; **50**(11):1785–1791.
16. Davila J, Fridman L, Levant A. Observation and identification of mechanical systems via second order sliding modes. *International Journal of Control* 2006; **79**(10):1251–1262.
17. Hautus M. Strong detectability and observers. *Linear Algebra and its Applications* 1983; **50**:353–368.
18. Gessow A, Myers GC. *Aerodynamics of the Helicopter*. F. Ungar: New York, 1967.
19. Johnson W. *Helicopter Theory*. Dover: New York, 1994.
20. Gomes S, Ramos J. Airship dynamic modeling for autonomous operation. *IEEE International Conference on Robotics and Automation* (*ICRA'98*), Leuven, Belgium, 1998.
21. Bouabdallah S, Murrieri P, Siegwart R. Design and control of an indoor micro quadrotor. *IEEE International Conference on Robotics and Automation* (*ICRA'04*), New Orleans, U.S.A., 2004.
22. Mistler V, Benallegue A, M'Sirdi NK. Exact linearization and non-interacting control of a 4 rotors helicopter via dynamic feedback. *Preprints of the 10th IEEE International Workshop on Robot–Human Interactive Communication* (*Roman 2001*), Paris, 2001.
23. Slotine JJE. Sliding controller design for nonlinear systems. *International Journal of Control* 1984; **38**(2):465–492.
24. Slotine JJE, Hedrick JK, Misawa EA. On sliding observers for nonlinear systems. *Journal of Dynamic Systems, Measurement and Control* 1987; **109**:245–257.
25. Farell JA, Givargis TD, Barth MG. Real-time differential carrier phase GPS-aided INS. *IEEE Transactions on Control Systems Technology* 2000; **8**(4):709–721.
26. Filippov A. *Differential Equations with Discontinuous Right-hand Sides*. Kluwer Academic Publishers: Dordrecht, 1988.
27. Utkin V. *Sliding Modes in Control and Optimization*. Springer: London, 1992.

DOI: 10.1002/rnc